Available online at www.sciencedirect.com
ScienceDirect
Journal of Organometallic Chemistry 692 (2007) 755–760
Journal of Organometallic Chemistry
www.elsevier.com/locate/jorganchem

Synthesis, structure and electrochemistry of cationic diruthenium complexes of the type $[(N\cap N)_2Ru_2(CO)_2(\mu\text{-}CO)_2(\mu\text{-}OOCFc)]^+$ containing a ferrocenecarboxylato bridge and two chelating aromatic diimine ligands

Mathieu Auzias [a], Bruno Therrien [a], Georg Süss-Fink [a,*], Petr Štěpnička [b,*], Jiří Ludvík [c]

[a] Institut de Chimie, Université de Neuchâtel, Case postale 158, Avenue de Bellevaux 51, CH-2009 Neuchâtel, Switzerland
[b] Charles University, Faculty of Science, Department of Inorganic Chemistry, Hlavova 2030, CZ-12840 Prague 2, Czech Republic
[c] J. Heyrovský Institute of Physical Chemistry, Academy of Sciences of the Czech Republic, olejškova 3, CZ-18223 Prague, Czech Republic

Received 21 August 2006; received in revised form 29 September 2006; accepted 2 October 2006
Available online 18 October 2006

Abstract

The dinuclear bis(ferrocenecarboxylato) complex $Ru_2(CO)_4(\mu\text{-}OOCFc)_2(py)_2$ (Fc = ferrocenyl, py = pyridine) was found to react with aromatic diimines (2,2′-dipyridyl, 4,4′-dimethyl-2,2′-dipyridyl, 1,10-phenanthroline, 5-nitro-1,10-phenanthroline, and 5-amino-1,10-phenanthroline) in methanol to give the cationic diruthenium complexes $[(N\cap N)_2Ru_2(CO)_2(\mu\text{-}CO)_2(\mu\text{-}OOCFc)]^+$ (**1**: N∩N = 2,2′-dipyridyl, **2**: N∩N = 4,4′-dimethyl-2,2′-dipyridyl, **3**: N∩N = 1,10-phenanthroline, **4**: N∩N = 5-nitro-1,10-phenanthroline, **5**: N∩N = 5-amino-1,10-phenanthroline), which have been isolated as the hexafluorophosphate salts. The molecular structure of **3**, solved by single-crystal X-ray analysis of the tetraphenylborate salt [**3**][BPh_4], shows a diruthenium backbone bridged by two carbonyl and by one ferrocenecarboxylato ligand, the two 1,10-phenanthroline ligands being in the axial positions. Cyclic voltammetry in dichloromethane reveals for all compounds two successive oxidations due to ferrocene/ferrocenium redox couple and oxidation of the diruthenium core.

Keywords: Carbonyl ligands, Carboxylato ligands; Ferrocenyl substituents; Diimine ligands; Dinuclear complexes; Ruthenium; Electrochemistry

1. Introduction

Sawhorse-type ruthenium complexes are well-known since 1969, when Lewis and co-workers [1] reported the formation of $[Ru_2(CO)_4(\mu\text{-}OOCR)_2]_n$ polymers by refluxing suspensions of $Ru_3(CO)_{12}$ in the corresponding carboxylic acid and depolymerisation of these materials in coordinating solvents to give dinuclear complexes of the type $Ru_2(CO)_4(\mu\text{-}OOCR)_2L_2$, L being acetonitrile, pyridine or another two-electron donor. These dinuclear complexes have been shown later, by a single-crystal X-ray structure analysis of $Ru_2(CO)_4(\mu\text{-}OOCBu^n)_2(P^tBu_3)_2$ to have a $Ru_2(CO)_4$ backbone in a sawhorse-type arrangement with two $\mu\text{-}\eta^2$-carboxylato bridges and two axial phosphane ligands [2]. In the meantime, a considerable number of such sawhorse-type diruthenium complexes with carboxylato [3], carboxamido [4], phosphinato [5], sulfonato [6], pyrazolato [7] or oximato [8] bridges have been synthesised and used in catalysis [8,9] or for the assembly of mesomorphic materials [10].

Cationic diruthenium complexes of the type $[(N\cap N)_2Ru_2(CO)_2(\mu\text{-}CO)_2(\mu\text{-}OOR)]^+$ have been synthesised reacting directly $[Ru_2(CO)_4(\mu\text{-}OOCR)_2]_n$ polymers with diimines [11], and this type of complexes has been studied in catalysis for hydrogenation [12] and hydroformylation [13]. Recently, Spiccia and co-workers reported the reaction

* Corresponding authors. Tel.: +41 32 718 2499; fax: +41 32 718 2511.
E-mail addresses: georg.suess-fink@unine.ch (G. Süss-Fink), stepnic@natur.cuni.cz (P. Štěpnička).

0022-328X/$ - see front matter © 2006 Elsevier B.V. All rights reserved.
doi:10.1016/j.jorganchem.2006.10.019

of the sawhorse complexes $Ru_2(CO)_4(\mu\text{-}OOCR)_2(py)_2$ (R = Me, Ph) with diimines to give cationic diruthenium complexes of the type $[(N\cap N)_2Ru_2(CO)_2(\mu\text{-}CO)_2(\mu\text{-}OOR)]^+$ (N∩N = 2,2′-bipyridine and 1,10-phenanthroline) [14]. We applied this reaction also to the ferrocenyl-containing sawhorse-type complex $Ru_2(CO)_4(\mu\text{-}OOCFc)_2(py)_2$ (Fc = ferrocenyl) that we had obtained recently [15], in order to access cationic diruthenium ferrocene complexes with potentially interesting redox properties.

2. Results and discussion

Dodecacarbonyltriruthenium reacts first with ferrocenecarboxylic acid in refluxing tetrahydrofuran to give, in the presence of pyridine, the yellow crystalline dinuclear complex $Ru_2(CO)_4(\mu\text{-}\eta^2\text{-}OOCFc)_2(py)_2$. This complex reacts then in methanol (40 °C) with aromatic diimines to give the cationic diruthenium complexes $[(N\cap N)_2Ru_2(CO)_2(\mu\text{-}CO)_2(\mu\text{-}OOCFc)]^+$ (**1**: N∩N = 2,2′-dipyridyl, **2**: N∩N = 4,4′-dimethyl-2,2′-dipyridyl, **3**: N∩N = 1,10-phenanthroline, **4**: N∩N = 5-nitro-1,10-phenanthroline, **5**: N∩N = 5-amino-1,10-phenanthroline), isolated as the hexafluorophosphate salts. Compounds [**1**–**5**][PF_6] are obtained as air-stable orange-brown powders, which have been unambiguously characterised by their IR, NMR and MS data as well as by correct micro-analytical data (see Section 3). Since only poor quality crystals were obtained from the hexafluorophosphate salts, we reacted [**3**][PF_6] in acetone with $NaBPh_4$, which yielded crystals of [**3**][BPh_4] suitable for X-ray analysis.

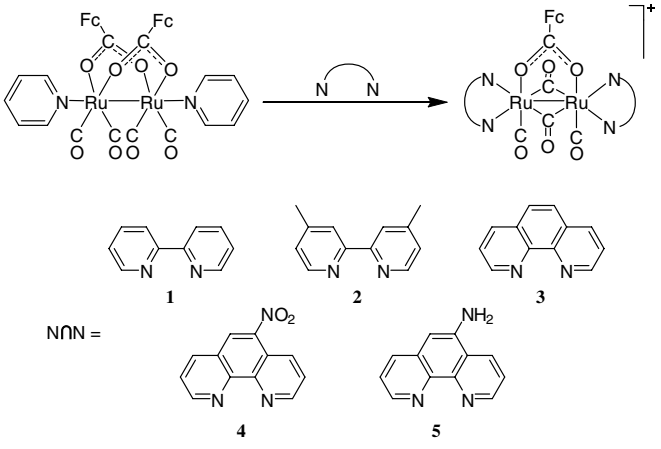

The single-crystal structure analysis of [**3**][BPh_4] shows an edge-sharing bioctahedral configuration for the ruthenium atoms with the two 1,10-phenanthroline ligands occupying the axial positions (Fig. 1). Selected bond lengths and angles are presented in Table 1. The Ru–Ru distances [2.6979(4) Å] are in the range of a ruthenium–ruthenium single bond, as it was also observed in analogous cationic complexes; $[(N\cap N)_2Ru_2(CO)_2(\mu\text{-}CO)_2(\mu\text{-}OOCH_3)]^+$ (N∩N = 2,2′-dipyridyl) [16], (N∩N = 1,10-phenanthroline) [11], and (N∩N = di(2-pyridyl)amine) [17]. The two axial 1,10-phenanthroline ligands are not coplanar with the $Ru_2(\mu\text{-}CO)_2$ core, the angle between the two phenanthroline planes being 32.54(6)°. These phenanthroline ligands are involved in slipped-parallel π–π stacking interactions with neighbouring cations, thus forming columnar multimer of cations along the crystallographic *a* axis (Fig. 2). The shortest centroid···centroid distance observed between the π-stacked interacting systems (3.52 Å) is in good agreement with the theoretical value calculated for this π-stacking mode [18]. The tetraphenylborate anions and acetone molecules are intercalated between these cationic multimers.

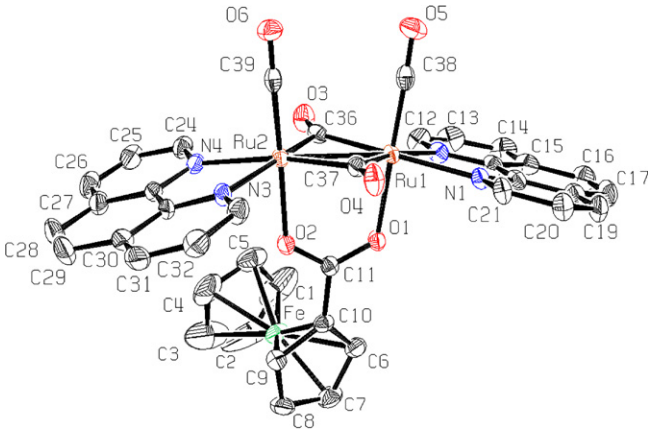

Fig. 1. Molecular structure of the $[Ru_2(CO)_2(\mu\text{-}CO)_2(\mu\text{-}OOCFc)(1,10\text{-phenantroline})_2]^+$ cation (**3**). Hydrogen atoms, tetraphenylborate anion and acetone molecule have been omitted for clarity.

Table 1
Selected bond lengths (Å) and angles (°) for [**3**][BPh_4]

Interatomic distances (Å)			
Ru(1)–N(1)	2.196(3)	Ru(1)–N(2)	2.211(3)
Ru(2)–N(3)	2.188(3)	Ru(2)–N(4)	2.200(3)
Ru(1)–O(1)	2.121(2)	Ru(2)–O(2)	2.084(2)
Ru(1)–C(38)	1.845(4)	Ru(2)–C(39)	1.856(4)
O(1)–C(11)	1.280(4)	O(2)–C(11)	1.274(4)
O(3)–C(36)	1.181(4)	O(4)–C(37)	1.182(4)
O(5)–C(38)	1.160(5)	O(6)–C(39)	1.153(5)
Ru(1)–Fe	5.6784(7)	Ru(2)–Fe	5.3334(7)
Ru(1)–Ru(2)	2.6979(4)		
Bond angles (°)			
Ru(1)–C(36)–Ru(2)	83.70(14)	Ru(1)–C(37)–Ru(2)	83.85(15)
Ru(1)–C(38)–O(5)	178.5(4)	Ru(2)–C(39)–O(6)	178.4(3)
C(36)–Ru(1)–C(37)	95.49(14)	C(36)–Ru(2)–C(37)	95.74(15)
N(1)–Ru(1)–N(2)	75.35(11)	N(3)–Ru(2)–N(4)	75.78(11)
O(1)–Ru(1)–C(38)	178.83(12)	O(2)–Ru(2)–C(39)	177.36(13)
O(1)–C(11)–O(2)	124.4(3)		

The presence of a ferrocenecarboxylato bridge with intramolecular Fe–Ru separations of about 5.5 Å makes **1**–**5** interesting substrates for electrochemical studies. The electrochemical behaviour of **1**–**5** was studied in the region of positive potentials by cyclic voltammetry on a platinum disc electrode and by voltammetry at a rotating platinum disc electrode (RDE) using dichloromethane solutions

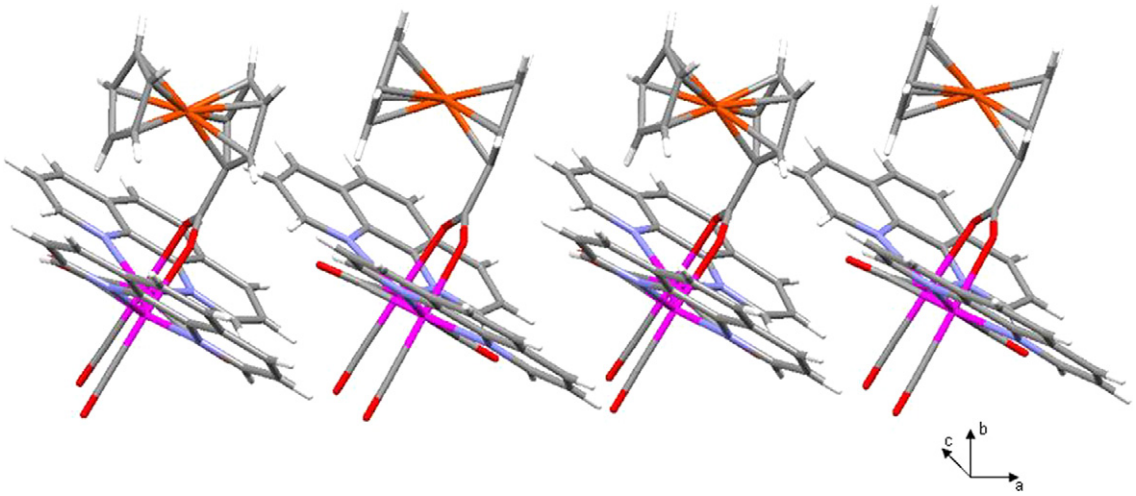

Fig. 2. Columnar multimers of **3** along the *a* axis.

containing $[Bu_4N][PF_6]$ as the supporting electrolyte. The data are summarised in Table 2.

The simplest compound in the series, **1** undergoes two successive oxidations within the experimentally accessible region (Fig. 3a). On the cyclic voltammogram, the first oxidation is electrochemically fully reversible, showing (when the switching potential is set before the second oxidation; see also below) the i_{pc}/i_{pa} ratio close to unity, $i_{pa} \propto v^{1/2}$ and $\Delta E_p = 70$ mV (i_{pa} and i_{pc} denote anodic and cathodic peak currents, respectively, and v is the scan rate), whilst the second anodic process is irreversible at all scan rates used (20–500 mV s^{-1}) while remaining diffusion-controlled ($i_{pa} \propto v^{1/2}$). The height of the second wave is nearly double of that of the first one, indicating a two-electron nature of the second oxidation. The results obtained by cyclic voltammetry fully correspond with voltammetric experiments at RDE which reveal two consecutive waves of which the second one is influenced by some chemical complications. The limiting current of the second wave decreases with decreasing scan rate and with increasing switching potential, which indicates a slow follow-up chemical reaction resulting into a formation of a layer (most likely polymeric one) covering the electrode surface. Considering the properties of the observed redox processes and the number of exchanged electrons, the first reversible process can be clearly attributed to ferrocene/ferrocenium couple and the wave at more positive potentials to an irreversible oxidation of the diruthenium core.

Table 2
Cyclic voltammetric data for **1**–**5**[a]

Compound	$E^{\circ'}$ (V)	ΔE_p (mV)
1	0.22	70
	0.82[b]	–
2	0.20	75
	0.76[b]	–
3	0.24	70
	0.82[b]	–
4	0.21	90[c]
	0.77[b]	–
	1.08[b]	–
5	0.22	95[c]
	0.88[b]	–

[a] Cyclic voltammograms were recorded at platinum disc electrode on ca. 5×10^{-4} M dichloromethane solutions containing 0.1 M Bu_4NPF_6 as the supporting electrolyte at room temperature. The potentials are given relative to ferrocene/ferrocenium reference. Definitions: formal redox potential $E^{\circ'} = 1/2(E_{pa} + E_{pc})$; separation of the cyclovoltammetric peaks $\Delta E_p = E_{pa} - E_{pc}$. E_{pa} and E_{pc} denote the anodic and cathodic peak potentials, respectively. The quoted values were obtained at the scan rate $v = 100$ mV/s.

[b] Irreversible process; E_{pa} given.

[c] Only the first oxidation couple recorded. ΔE_p increases when the whole range is scanned.

A strong support for this assignment comes from a comparison with complex **2** which shows very similar response in cyclic voltammetry and voltammetry at RDE but with the ferrocene- and ruthenium-centred oxidations shifted to less positive potentials by 20 mV and 60 mV, respectively. The shifts apparently reflect the presence of the electron-donating substituents (methyl groups) in positions 4,4′ of the bipyridyl ligands as well as their different distance from the respective redox centres.

In contrast to **1**, the limiting current due to the second wave in voltammetry at Pt-RDE remains constant with changing the scan rate (10 → 100 mV s^{-1}) for **2**, indicating that no coverage of the electrode surface occurs in the latter case. Such a different behaviour likely reflects the structural change as the methyl groups in positions 4,4′ at the bipyridyl obstruct the possible oxidative oligo-/polymerisation of the aromatic rings.

As for the compounds with 1,10-phenanthroline ligands, the redox behaviour of **3** featuring unsubstituted phenanthroline closely parallels that of **1** and **2** (see Table 2). The limiting current of the second wave in the RDE voltammogram depends only slightly on the scan rate and, hence, only a very limited formation of a layer covering the electrode surface can be expected.

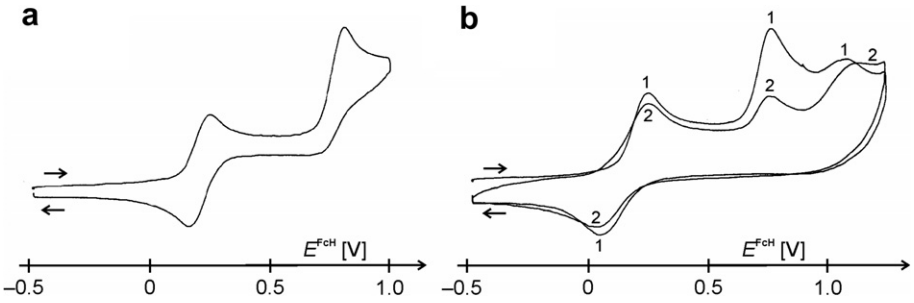

Fig. 3. Cyclic voltammograms of **1** (a) and **5** (b) as recorded at 100 mV s^{-1} scan rate on platinum disc electrode for ca. 5×10^{-4} M analyte solutions in dichloromethane solutions containing Bu_4NPF_6 as the supporting electrolyte (0.1 M). For **5**, the numerals indicate the scan numbers.

The introduction of nitro and amino groups onto the phenanthroline ligand results in considerable changes in the voltammograms, indicating a more complex electro-oxidation reaction scheme. Although the oxidation of **4** and **5** still proceeds in two well-separated steps assignment of which is the same as in the previous cases, properties of the individual redox steps differ from those mentioned above.

The oxidation of **4** and **5** starts with the ferrocene redox couple which appears at nearly the same potential as in all previous cases. It is evident that the ferrocene moiety is in fact electronically isolated from the diimine ligands where all structural changes occur. In both cases, however, the ferrocene/ferrocenium couple exhibits a higher anodic/cathodic peak separation in cyclic voltammograms (90–95 mV), which further increases when the switching potential is raised positively so that the scan involves both redox processes (see Fig. 3b). In addition, the shape of the cyclic voltammetric curve is changed towards sigmoidal.

The second oxidation processes occur as irreversible peaks of symmetric shape that points to strong surface phenomena being involved. Their potential is influenced by the phenanthroline substituents: The nitro group in **4** shifts the potential 60 mV positively while the amino group in **5** makes the oxidation by about 50 mV easier (both in comparison with **3**). Notably, the dependence of the peak current for the second peak on $v^{1/2}$ in cyclic voltammetry is linear only up to scan rate 50–100 mV s^{-1} while, at higher scan rates (200 and 500 mV s^{-1}), it shows a tendency to approach a constant value. In voltammograms at Pt-RDE of **4** and **5**, the second wave is observed only as a peak (i.e., without reaching a limiting current) whose height peak rapidly decreases with decreasing scan rate. For instance, the second wave disappears completely at 10 mV s^{-1} for **4**, whereas for **5** at the same scan rate the current even drops at potentials where the second wave in the cyclic voltammogram occurs. All this indicates that the electrode is blocked with a polymeric film at potentials of the core oxidation (though to a different degree). Compound **5** exhibits one more oxidation peak about 300 mV, which is probably due to the oxidation of the amino group.

It is also noteworthy that when only the first, reversible ferrocene/ferrocenium redox couple is recorded using cyclic voltammetry, the cathodic/anodic peak current ratio (i_{pc}/i_{pa}) equals to one for all studied compounds. However, when the cyclic voltammogram of **1**, **3**, and **4** is recorded over the whole potential range, i.e. including the second oxidation step, the cathodic peak current at the backward scan is by 5–20% higher than the anodic. The only exception is complex **2** which showed i_{pc}/i_{pa} ratio close to unity at all scan rates applied (note: **5** was difficult to compare with other member of the series due to a different overall oxidation pattern). This observation correlates with the extent of the electrode coverage as observed in voltammetry at RDE (see above) and further points to a catalytic reaction to be involved.

The interpretation most consistent with the observed data are that the film formed at the electrode during the forward scan is (partly) catalytically reduced during the back scan with the ferrocene/ferrocenium couple. As a result, the catalytic reductive destruction (desorption) of the polymeric film is achieved, which manifests itself with a partial regeneration of the electrode properties in repeated CV. This in turn indicates that the redox-induced structural changes do not lead to a disintegration of the complex molecule.

3. Experimental

3.1. General comments

All reagents were purchased either from Aldrich, Fluka or Acros and used without further purification. All manipulations were carried out by routine under nitrogen atmosphere. Organic solvents were degassed and saturated with nitrogen prior to use, methanol of HPLC grade was used. Dodecacarbonyltriruthenium [19] and $Ru_2(CO)_2(\mu\text{-}CO)_2(OOCFc)_2(py)_2$ [15] were prepared according to published methods. NMR spectra were recorded on a Varian 200 MHz spectrometer. IR spectra were recorded on a Perkin–Elmer 1720X FT-IR spectrometer (4000–400 cm^{-1}). Microanalyses were performed by the Laboratory of Pharmaceutical Chemistry, University of Geneva (Switzerland). Electro-spray mass spectra were obtained in positive-ion mode with a LCQ Finnigan mass spectrometer.

3.2. General synthesis of complexes [1–5][PF_6]

$Ru_2(CO)_4(OOCFc)_2(py)_2$ (100 mg, 0.1 mmol) and the corresponding diimine (0.4 mmol) were suspended in methanol (30 mL) in a Schlenk tube under nitrogen. The suspension was sonicated for 5 min and the solution was stirred at 40 °C for 24 h. The precipitation of a fine yellow-orange (complexes **1**–**3**) or brown (complexes **4** and **5**) powder was induced by addition of potassium hexafluorophosphate, this powder was collected and washed with cold ethanol and diethyl ether before being dried.

Data for [(2,2′-dipyridyl)$_2$$Ru_2(CO)_2$(μ-CO)$_2$(μ-OOCFc)][$PF_6$] (**1**): Yield: 86 mg, 93%. ^{1}H NMR (d_6-acetone): 10.37 (d, 4H, H_A, $^3J = 5.6$ Hz); 9.00 (d, 4H, H_D, $^3J = 8$ Hz); 8.61 (t, 4H, H_C, $^3J = 7.6$ Hz, $^3J = 15.6$ Hz); 8.28 (t, 4H, H_B, $^3J = 5.6$ Hz, $^3J = 13.2$ Hz); 3.92 (t, 2H, H_{Cp}, $^3J = 2$ Hz, $^3J = 4$ Hz); 3.57 (s, 5H, H_{Cp}); 3.52 (t, 2H, H_{Cp}, $^3J = 2$ Hz, $^3J = 4$ Hz). ESI-MS: *m*/*z* 856.8. IR (KBr): 3117, 3087, 2853, 2017, 1993, 1808, 1736, 1602, 1526, 1488, 1479, 1443, 1398, 1385, 1362, 1325 cm^{-1}. Anal. Calc. for $C_{35}H_{25}FeO_6N_4PF_6Ru_2$ (1000.55): C, 41.65; H, 2.47; N, 5.40. Found: C, 42.01; H, 2.52; N, 5.60%.

Data for [(4,4′-dimethyl-2,2′-dipyridyl)$_2$$Ru_2(CO)_2$(μ-CO)$_2$(μ-OOCFc)][$PF_6$] (**2**): Yield: 83 mg, 85%. ^{1}H NMR (CD_2Cl_2): 10.14 (d, 4H, H_A, $^3J = 5.6$ Hz); 8.74 (s, 4H, H_C); 7.80 (d, 4H, H_B, $^3J = 4.8$ Hz); 3.89 (t, 2H, H_{Cp}, $^3J = 2$ Hz, $^3J = 4$ Hz); 3.58 (t, 2H, H_{Cp}, $^3J = 2$ Hz, $^3J = 4$ Hz); 3.56 (s, 5H, H_{Cp}). ESI-MS: *m*/*z* 912.8. IR (KBr): 3077, 2928, 2017, 1960, 1799, 1732, 1617, 1513, 1488, 1396, 1360, 1316, 1295, 1240 cm^{-1}. Anal. Calc. for $C_{39}H_{33}FeO_6N_4PF_6Ru_2$ (1056.65): C, 44.33; H, 3.15; N, 5.30. Found: C, 44.20; H, 2.91; N, 4.96%.

Data for [(1,10-phenanthroline)$_2$$Ru_2(CO)_2$(μ-CO)$_2$(μ-OOCFc)][$PF_6$] (**3**): Yield: 77 mg, 79%. ^{1}H NMR (d_6-acetone): 10.70 (d, 4H, H_A, $^3J = 5$ Hz); 8.90 (d, 4H, H_C, $^3J = 8.2$ Hz); 8.38 (m, 8H, $H_{B–D}$); 3.71 (t, 2H, H_{Cp}, $^3J = 2$ Hz, $J = 4$ Hz); 3.51 (s, 5H, H_{Cp}); 3.19 (t, 2H, H_{Cp}, $^3J = 2$ Hz, $^3J = 4$ Hz). ESI-MS: *m*/*z* 904.8. IR (KBr): 3081, 2016, 1984, 1802, 1734, 1629, 1587, 1511, 1485, 1434, 1396, 1385, 1360, 1318, 1225 cm^{-1}. Anal. Calc. for $C_{39}H_{25}FeO_6N_4PF_6Ru_2$ (1051.79): C, 44.67; H, 2.40; N, 5.34. Found: C, 44.46; H, 2.50; N, 5.13%.

Data for [(5-nitro-1,10-phenanthroline)$_2$$Ru_2(CO)_2$(μ-CO)$_2$(μ-OOCFc)][$PF_6$] (**4**): Yield: 80 mg, 75%. ^{1}H NMR (d_6-acetone): 10.90 (t, 4H, $H_{A–B}$, $^3J = 5$ Hz, $^3J = 10$ Hz); 9.68 (d, 2H, H_C, $^3J = 7.6$ Hz); 9.50 (d, 4H, $H_{F–G}$, $^3J = 5$ Hz); 8.84 (m, 4H, $H_{D–E}$); 3.73 (t, 2H, H_{Cp}, $^3J = 2$ Hz, $^3J = 4$ Hz); 3.54 (s, 5H, H_{Cp}); 3.20 (t, 2H, H_{Cp}, $^3J = 2$ Hz, $^3J = 4$ Hz). ESI-MS : *m*/*z* 993.8. IR (KBr): 3082, 2014, 1987, 1808, 1737, 1630, 1586, 1538, 1506, 1483, 1434, 1396, 1385, 1361, 1345, 1298 cm^{-1}. Anal. Calc. for $C_{39}H_{23}FeO_{10}N_6PF_6Ru_2$ (1138.58): C, 41.44; H, 2.04; N, 7.38. Found: C, 41.62; H, 2.22; N, 6.98%.

Data for [(5-amino-1,10-phenanthroline)$_2$$Ru_2(CO)_2$(μ-CO)$_2$(μ-OOCFc)][$PF_6$] (**5**): Yield: 53 mg, 53%. ^{1}H NMR (d_6-acetone): 10.71 (d, 2H, H_A, ^{3}J = 4.8 Hz); 10.31 (d, 2H, H_G, $^3J = 4.8$ Hz); 9.36 (d, 2H, H_C, $^3J = 8.6$ Hz); 8.73 (d, 2H, H_E, $^3J = 8.2$ Hz); 8.58 (dd, 2H, H_B, $^3J = 5.2$ Hz, $^3J = 8.6$ Hz); 8.32 (dd, 2H, H_B, $^3J = 5$ Hz, $^3J = 8.2$ Hz); 7.44 (s, 2H, H_D); 6.49 (s, 4H, NH_2); 3.76 (t, 2H, H_{Cp}, $^3J = 2$ Hz, $^3J = 4$ Hz); 3.55 (s, 5H, H_{Cp}); 3.20 (t, 2H, H_{Cp}, $^3J = 2$ Hz, $^3J = 4$ Hz). ESI-MS: *m*/*z* 934.9. IR (KBr): 3081, 2924, 2013, 1980, 1803, 1737, 1639, 1598, 1489, 1464, 1428, 1397, 1385, 1280 cm^{-1}. Anal. Calc. for $C_{39}H_{27}FeO_6N_6PF_6Ru_2$ (1078.62): C, 43.43; H, 2.52; N, 7.79. Found: C, 43.12; H, 2.21; N, 7.37%.

3.3. Electrochemistry

Electrochemical measurements were performed on a multipurpose polarograph PA3 interfaced to a Model 4103 XY recorded (both Laboratorní přístroje, Prague) at room temperature using a standard three-electrode cell: rotating (RFE) or stationary platinum disc (1 mm diameter) working electrode, platinum wire auxiliary electrode, and saturated calomel electrode (SCE) reference electrode, separated from the analysed solution by a salt bridge filled with 0.1 M Bu_4NPF_6 in dichloromethane. The samples were dissolved in dichloromethane (Merck p.a.) to give ca. 5×10^{-4} M concentration of the analyte and 0.1 M [Bu_4N][PF_6] (Fluka, puriss for electrochemistry). The solutions were degassed with argon prior to the measurement and then kept under an argon blanket. Cyclic voltammograms were recorded at stationary platinum disc electrode (scan rates 20–500 mV/s), whereas the voltammograms were obtained at RDE (500 rpm, scan rates 10–100 mV/s). The platinum disk was mechanically cleaned after every experiment to achieve reproducible results. Redox potentials given are given relative to the ferrocene/ferrocenium couple.

3.4. Structure determination

X-ray data for [**3**][BPh_4]·$(CH_3)_2CO$; $C_{66}H_{51}BFeN_4O_7Ru_2$, $M = 1280.91$ g mol^{-1}, orthorhombic, *Pbca* (no. 61), $a = 13.6825(7)$ Å, $b = 22.8306(12)$ Å, $c = 35.4690(16)$ Å, $V = 11079.8(10)$ Å^3, $T = 173$ K, $Z = 8$, μ (Mo–Kα) = 0.857 mm^{-1}, 10 785 reflections measured, 6919 unique ($R_{int} = 0.1590$) which were used in all calculations. The final wR (F^2) was 0.0959 (all data). The data were measured using a Stoe Image Plate Diffraction system equipped with a ϕ circle, using Mo Kα graphite-monochromated radiation ($\lambda = 0.71073$ Å) with ϕ range 0–100°, increment of 0.8°, 10 min per frame, 2θ range from 2.0° to 26°, D_{max}–D_{min} = 12.45–0.81 Å. The structure was solved by direct methods using the program SHELXS-97 [20]. The refinement and all further calculations were carried out using SHELXL-97 [21]. The H-atoms were included in calculated positions and treated as riding atoms using the SHELXL default parameters. The non-H atoms were refined anisotropically, using weighted full-matrix least-square on F^2. Fig. 1 is drawn with ORTEP [22] and Fig. 2 with MERCURY [23].

Appendix A. Supplementary material

CCDC 615991 contains the supplementary crystallographic data for [**3**][BPh_4]·$(CH_3)_2CO$. These data can be obtained free of charge via http://www.ccdc.cam.ac.uk/conts/retrieving.html, or from the Cambridge Crystallographic Data Centre, 12 Union Road, Cambridge CB2 1EZ, UK; fax: (+44) 1223-336-033; or e-mail: deposit@ccdc.cam.ac.uk. Supplementary data associated with this article can be found, in the online version, at doi:10.1016/j.jorganchem.2006.10.019.

References

[1] G.R. Crooks, B.F.G. Johnson, J. Lewis, I.G. Williams, G. Gamlen, J. Chem. Soc. A (1969) 2761.
[2] H. Schumann, J. Opitz, J. Pickardt, J. Organomet. Chem. 128 (1977) 253.
[3] (a) M. Bianchi, P. Frediani, U. Matteoli, G. Menchi, F. Piacenti, G. Petrucci, J. Organomet. Chem. 259 (1983) 207;
(b) M. Rotem, Y. Shvo, I. Goldberg, U. Shmueli, Organometallics 3 (1984) 1758;
(c) G. Süss-Fink, G. Herrmann, P. Morys, J. Ellermann, A. Veit, J. Organomet. Chem. 284 (1985) 263;
(d) M. Rotem, I. Goldberg, U. Shmueli, Y. Shvo, J. Organomet. Chem. 314 (1986) 185;
(e) S.J. Sherlock, M. Cowie, E. Singleton, M.M. de V. Steyn, Organometallics 7 (1988) 1663;
(f) G.F. Schmidt, G. Süss-Fink, J. Organomet. Chem. 362 (1989) 179;
(g) G. Süss-Fink, J.L. Wolfender, F. Neumann, H. Stoeckli-Evans, Angew. Chem., Int. Ed. Engl. 29 (1990) 429;
(h) D.S. Bohle, H. Vahrenkamp, Inorg. Chem. 29 (1990) 1097.
[4] F. Neumann, H. Stoeckli-Evans, G. Süss-Fink, J. Organomet. Chem. 379 (1989) 139.
[5] D.S. Bohle, H. Vahrenkamp, Inorg. Chem. 29 (1990) 1097.
[6] G. Rheinwald, H. Stoeckli-Evans, G. Süss-Fink, J. Organomet. Chem. 441 (1992) 295.
[7] (a) F. Neumann, G. Süss-Fink, J. Organomet. Chem. 367 (1989) 175;
(b) F. Neumann, H. Stoeckli-Evans, G. Süss-Fink, J. Organomet. Chem. 379 (1989) 151.
[8] M. Langenbahn, H. Stoeckli-Evans, G. Süss-Fink, Helv. Chim. Acta 74 (1991) 549.
[9] (a) J. Jenck, P. Kalck, E. Pinelli, M. Siani, A. Thorez, J. Chem. Soc., Chem. Commun. (1988) 1428;
(b) J.L. Wolfender, F. Neumann, G. Süss-Fink, J. Organomet. Chem. 389 (1990) 351;
(c) A. Salvini, P. Frediani, C. Giannelli, L. Rosi, J. Organomet. Chem. 690 (2005) 371.
[10] R. Deschenaux, B. Donnio, G. Rheinwald, F. Stauffer, G. Süss-Fink, J. Velker, J. Chem. Soc., Dalton Trans. (1997) 4351.
[11] P. Frediani, M. Bianchi, A. Salvini, R. Guarducci, L.C. Carluccio, F. Piacenti, S. Ianelli, M. Nardelli, J. Organomet. Chem. 463 (1993) 187.
[12] (a) P. Frediani, M. Bianchi, A. Salvini, R. Guarducci, L.C. Carluccio, F. Piacenti, J. Organomet. Chem. 498 (1995) 187;
(b) A. Salvini, P. Frediani, E. Rivalta, Inorg. Chim. Acta 351 (2003) 225.
[13] P. Frediani, M. Bianchi, A. Salvini, L.C. Carluccio, L. Rosi, J. Organomet. Chem. 547 (1997) 35.
[14] P. Pearson, C.M. Kepert, G.B. Deacon, L. Spiccia, A.C. Warden, B.W. Skelton, A.H. White, Inorg. Chem. 43 (2004) 683.
[15] M. Auzias, B. Therrien, G. Labat, H. Stoeckli-Evans, G. Süss-Fink, Inorg. Chim. Acta 359 (2006) 1012.
[16] M.M. de V. Steyn, E. Singleton, Acta Crystallogr., Sect. C 44 (1988) 1722.
[17] C.M. Kepert, G.B. Deacon, L. Spiccia, Inorg. Chim. Acta 355 (2003) 213.
[18] S. Tsuzuki, K. Honda, T. Uchimura, M. Mikami, K. Tanabe, J. Am. Chem. Soc. 124 (2002) 104.
[19] H.D. Kaesz, Inorganic Synthesis, vol. 26, Wiley–Interscience, New York, 1989, p. 259.
[20] G.M. Sheldrick, Acta Crystallogr., Sect. A 46 (1990) 467.
[21] G.M. Sheldrick, SHELXL-97, University of Göttingen, Göttingen, Germany, 1999.
[22] L.J. Farrugia, J. Appl. Crystallogr. 30 (1997) 565.
[23] I.J. Bruno, J.C. Cole, P.R. Edgington, M. Kessler, C.F. Macrae, P. McCabe, J. Pearson, R. Taylor, Acta Crystallogr., Sect. B 58 (2002) 389.